A new insight into the work-of-indentation approach used in the evaluation of material's hardness from nanoindentation measurement with Berkovich indenter

ARTICLE *in* COMPUTATIONAL MATERIALS SCIENCE · APRIL 2014

Impact Factor: 2.13 · DOI: 10.1016/j.commatsci.2013.12.005

3 AUTHORS:

Kaushal K Jha
Florida International University
9 PUBLICATIONS **26** CITATIONS
SEE PROFILE

Nakin Suksawang
Florida Institute of Technology
23 PUBLICATIONS **103** CITATIONS
SEE PROFILE

Arvind Agarwal
Florida International University
213 PUBLICATIONS **3,838** CITATIONS
SEE PROFILE

Computational Materials Science 85 (2014) 32–37

Contents lists available at ScienceDirect

Computational Materials Science

journal homepage: www.elsevier.com/locate/commatsci

A new insight into the work-of-indentation approach used in the evaluation of material's hardness from nanoindentation measurement with Berkovich indenter

Kaushal K. Jha [a], Nakin Suksawang [b,*], Arvind Agarwal [c]

[a] Department of Civil and Environmental Engineering, Florida International University, Miami, FL 33174, USA
[b] Department of Civil Engineering, Florida Institute of Technology, Melbourne, FL 32901, USA
[c] Nanomechanics and Nanotribology Laboratory, Department of Mechanical and Materials Engineering, Florida International University, Miami, FL 33174, USA

ARTICLE INFO

Article history:
Received 10 June 2013
Received in revised form 22 November 2013
Accepted 2 December 2013

Keywords:
Elastic energy constant
Hardness
Nanoindentation
Oliver and Pharr method
Work-of-indentation approach

ABSTRACT

The work-of-indentation approach employed to extract the hardness of a material from the load–displacement data is often misinterpreted and improperly compared with the Oliver and Pharr method. A theoretical basis is presented to show that the hardness values evaluated using these two methods are fundamentally different, but are interrelated. As such, an expression that relates one type of hardness to another is derived by considering an energy-based relationship between the contact and the maximum penetration depths for an ideally sharp Berkovich indenter. This modified work-of-indentation approach is first validated using the load–displacement data obtained from the finite element simulation of the indentation contact performed with a Berkovich equivalent conical indenter on materials having a wide range of elastic recovery. The real load–displacement data – with and without dwelling – from ceramics oxides and metals corresponding to a peak indentation load lying in the range 20–120 mN are also considered to validate the proposed method. It has been found that a correction due to the amount of work done during dwelling is required if the load–displacement data also feature a dwelling phase. The hardness value so obtained is found to be in close agreement with its Oliver and Pharr analogue for each material considered thereby indicating that the modified approach, in the present form, is applicable even for blunt indenter when the tip radius is very small as compared to the maximum penetration depth. Further refinement of this methodology is, however, required to take the effect of material's pile-up, sink-in, and tip bluntness on the measured hardness into account.

1. Introduction

Hardness of a material may be extracted from the load–displacement curve obtained as an outcome of a nanoindentation experiment at least by two methods: the Oliver and Pharr (OP) procedure [1] and the work-of-indentation (WI) approach [2]. In the OP method, it is evaluated as the peak indentation load (P_{max}) divided by the projected contact area (A_c) of impression, which may be expressed as:

$$H_{OP} = \frac{P_{max}}{A_c(h_c)} = \frac{P_{max}}{\sum_{i=0}^{i=9} C_0 (h_c)^{2-i}} \quad (1)$$

where h_c denotes the contact depth. Constants C_i enclosed in the summation, except the first one, account for the roundness at the tip of the indenter. These constants are usually determined by fitting the plot between contact depth and contact area by a harmonic polynomial, called area function, of the form shown in the denominator of Eq. (1). For this purpose, a test material with known Young's modulus of elasticity is repeatedly indented up to a maximum depth of penetration of varying magnitude. While the contact depth is computed from the analytical derivative of the power law representing the unloading curve for each indent, the contact area is calculated from the Sneddon's solution [3] for indentation of elastic half-space by a rigid axisymmetric indenter. The constant C_0 depends on the indenter geometry; for a Berkovich indenter, it is equal to 24.56. For an ideally sharp pyramidal indenter, Eq. (1) has the following succinct form:

$$H_{OP} = \frac{P_{max}}{C_0 h_c^2}. \quad (2)$$

For many materials, the OP method provides reasonable estimate of hardness values. However, this method becomes cumbersome and time consuming when it is employed to determine the hardness of heterogeneous materials such as concrete, bone and shale. This is due to the fact that experiment on such material

* Corresponding author. Tel.: +1 321 674 7504; fax: +1 321 674 7565.
E-mail address: nsuksawang@fit.edu (N. Suksawang).

0927-0256/$ - see front matter © 2013 Elsevier B.V. All rights reserved.
http://dx.doi.org/10.1016/j.commatsci.2013.12.005

involves a massive array of continuous indentations in order to capture the mechanical properties of all constituents present in it [4]. As the tip of an indenter deteriorates with every indent, the area function described above would need to be updated at regular intervals to account for the changing tip condition. Furthermore, the OP method provides inaccurate hardness value for the material which exhibits excessive pile-up or sink-in during indentation.

The WI approach, on the other hand, utilizes the total work done (W_T) in indenting the material to a certain depth. Tuck et al. [2] derived the following relationship to determine the hardness of a material, which is, for the sake of comparison, denoted herein as H_N.

$$H_N = \frac{kP_{\max}^3}{9W_T^2} \tag{3}$$

where k $(= C_0^{-1})$ is a constant which takes indenter geometry into account; its value is 0.0408 and 0.0378 for Berkovich and Vickers indenters, respectively. There are two important advantages associated with the WI approach: (i) it does not require the evaluation of contact area at all; and (ii) the quantity W_T can be evaluated very precisely even if pile-up around the indenter is significant. Despite these advantages, mutually contradictory conclusions concerning the accuracy of this approach are often reported in the literature [5–9]. Since these studies are based on the responses from a very limited number of materials, drawing exact conclusion is extremely difficult. However, after a close review of these studies, one may tentatively conclude that WI and the OP procedures provide similar hardness for a material when it is less than or equal to 1GPa approximately, but their difference increases remarkably as a material gets harder. Again, some of the assumptions used in the WI approach appear to be misleading, which severely limit its domain of application. Tuck et al. [2], for instance, suggested that that the total work done in Eq. (3) may be replaced by the plastic work (W_P). These two parameters are interchangeable only for the perfectly plastic material in which case the recoverable deformation is either zero or negligibly small. Recently Xiang et al. [9] showed that both methods yield similar values of hardness for the component materials (NiO–YSZ, Ni–YSZ and YSZ) of Solid Oxide Fuel Cell (SOFCs). However, their derivation violates the notion of the total work done generally adopted in the indentation analysis. It should be noted that total work done is always evaluated as the area bounded by the loading curve up to the maximum depth of penetration, not the contact depth. Thus, a reappraisal of the WI approach becomes essential if the advantages associated with this particular method are to be exploited. As such, the aims of this study are twofold: (1) to gain further insight into the work-of-indentation approach by considering the load–displacement responses from a wide range of materials; and (2) to improve the existing approach so that the evaluation of hardness even for a relatively harder material (with $H > 1$ GPa) could be done with great accuracy. Toward this end, both simulated and instrumented indentation data [1,9,15,16] covering the hardness range of 0.21–35 GPa are utilized in this study.

2. Improved work-of-indentation approach

We begin our analysis of the existing work-of-indentation approach with a simple case involving an ideally sharp pyramidal indenter. When this condition prevails, the loading curve may be represented by a parabolic relation: $P = Ch^2$ such that $W_T = P_{\max}$-$h_{\max}/3$. On substitution, Eq. (3) simplifies to

$$H_N = \frac{P_{\max}}{C_0 h_{\max}^2} \tag{4}$$

Comparison of Eqs. (2) and (4) reveals that the hardness values determined by the OP method and WI approach differ in the choice of penetration depth. While the former uses the contact depth, the latter employs the maximum depth of penetration and, therefore, they are fundamentally different. Hardness evaluated by Eq. (4) is sometimes referred to as 'nominal hardness' of a material [10,11]. This subtlety between the nominal and the conventional hardness values has been completely overlooked in earlier studies. Here, for convenience, H_{OP} determined by the Oliver and Pharr method is referred to as the conventional hardness. It is evident from Eqs. (2) and (4) that the discrepancy in the hardness values for a given material evaluated by these two procedures depends on how far the contact and maximum penetration depths are located on the $P - h$ space (Fig. 1).

Attaf [12] derived an expression that relates contact depth with maximum depth of penetration, which may be expressed as:

$$h_c = \frac{2(\lambda_E - 1)}{(2\lambda_E - 1)} h_{\max} \tag{5}$$

where λ_E is the elastic energy constant [12,13] expressed as the ratio of elastic work to the absolute work of indentation. This absolute work is defined as the maximum energy that could be dissipated in a particular indentation experiment and is evaluated from the shaded area shown in Fig. 1. The elastic energy constant (λ_E) characterizes the response of a material to indentation and can take any value between 1 and ∞, where upper limit corresponds to the perfectly plastic material. In one of our recent studies [14], it has been shown that λ_E depends on the material properties as well as indenter tip radius to penetration depth ratio. Eq. (5) yields contact depth with the accuracy better than 95% as compared to its experimental analogue [9,12,13]. When λ_E tends to infinity, contact depth approaches the maximum penetration depth, thereby indicating that the nominal and conventional hardness values are almost equal. To explain how exactly the nominal and conventional hardness values deviate from each other, a closed form expression could be obtained for the case involving an ideally sharp indenter. Using Eqs. (2), (3), and (5), the following expression may be obtained,

$$K_N = \frac{H_{OP}}{H_N} = \frac{(2\lambda_E - 1)^2}{4(\lambda_E - 1)^2} \tag{6}$$

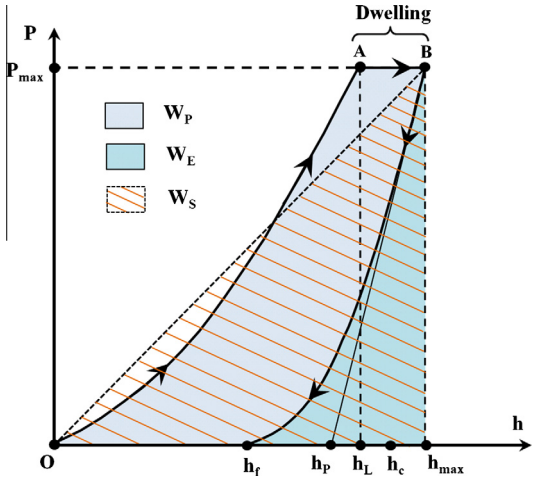

Fig. 1. Schematic representation of indentation load–displacement curves. Terms W_S, W_T, W_P and W_E describe the absolute, total, plastic and elastic work of indentation. Similarly, $P_{\max}$, $h_{\max}$, h_P, h_c and h_f, respectively, denote the peak indentation load, maximum depth of penetration, plastic, contact and residual depths. Symbol h_L describes the penetration depth at which the increase in loading ceases.

Fig. 2 shows the variation of hardness ratio as a function of the elastic energy constant (λ_E). It is apparent from the figure that the nominal and conventional hardness of a material are approximately equal if its λ_E value is greater than 10. The difference between H_N and H_{OP} tends to increase as λ_E approaches unity. This explains why the nominal hardness deviates so much from the conventional one when the material is harder than 1 GPa. Thus, to obtain a conventional hardness comparable to H_{OP} by the WI approach, Eq. (3) must be multiplied by the hardness correction factor K_N.

3. Verification and discussion

While deriving Eq. (6), the tip of the indenter is assumed perfectly sharp. In reality, no indenters are perfectly sharp as some roundness is inevitably present at the tip. Therefore, Eq. (6) is first validated using the load–displacement response obtained by the finite element simulation of the indentation process since a condition of perfectly sharp tip can be easily imposed. In the next, the real load–displacement data from metals and oxides of ceramics are considered to establish the extent to which a blunt indenter may be approximated as a perfectly sharp.

In this study, a commercially available software ABAQUS with large strain feature is used to simulate the elastoplastic indentation. A two-dimensional axisymmetric finite element model is used for the purpose in which the Berkovich indenter is modeled as a rigid conical indenter with half-included angle of 70.3°. Note that a conical indenter having this magnitude of half-included angle gives the same projected area-to-depth ratio as a Berkovich indenter. Selection of the specimen size is one of the most important steps in the modeling, as it governs the accuracy of the simulations. Poon et al. [15] showed that accurate load–displacement curves may be obtained if the specimen size satisfies the following convergence condition:

$$\frac{r_s}{h_s} \geqslant 1; \quad \frac{h_s}{h_{\max}} \geqslant 100 \tag{7}$$

where r_s and h_s are the radius and height of the cylindrical specimen, respectively. They are taken to be 30,000 nm, large enough to acquire an accurate load–displacement curve up to a penetration depth of 300 nm, as per the condition given by Eq. (7). Exploiting the advantage offered by the axisymmetric conditions, only half of the cross-section of the specimen and indenter are considered, as shown in Fig. 3. The entire domain is discretized using 4-node quadrilateral elements, with the highest mesh density in the vicinity of contact to account for large local deformation beneath the indenter similar to one adopted in Ref. [16]. Progressively coarser mesh is used as we move away from the contact resulting in 4097 elements and 4228 nodes.

The specimen is modeled as elasto-plastic deformable materials, which are assumed to obey the following bilinear stress (σ)-strain (ε) relations:

$$\sigma = \begin{cases} E_s\varepsilon & \text{for } \varepsilon \leqslant \sigma_y/E_s \\ \sigma_y + E_p(\varepsilon - \sigma_y/E) & \text{for } \varepsilon > \sigma_y/E_s \end{cases} \tag{8}$$

where E_s is the modulus of elasticity, σ_y is the yield strength and E_P is the work hardening parameter. The constitutive law given by Eq. (8) has been extensively used in the simulation of indentation by the finite element method [17–19]. Roller boundary conditions are applied along the axis of symmetry and the bottom of the specimen, as shown in Fig. 3. The contact surface is assumed to be rough with coefficient of friction equal to 0.4 in the model. While the Poisson's ratio is fixed at 0.25 in all simulations, the elastic modulus and the yield strength are systematically varied between 27–410 GPa and 1.6–14 GPa, respectively. Similarly, two cases of work hardening with E_P equal to 0 and 5 σ_y are considered. The model parameters are summarized in Table 1. This set of data provides the load–displacement curves with λ_E value falling in the range 1.85–15.2. Simulations are carried out in the displacement-controlled mode in which the indenter is pushed into the specimen up to a specified depth of 250 nm.

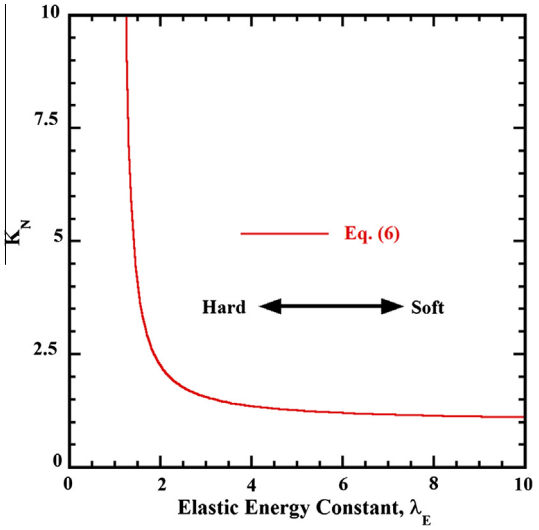

Fig. 2. Variation of hardness correction factor, K_N with elastic energy constant, λ_E .

Simulated load–displacement curves are analyzed by the aforementioned methods and results are compared as shown in Fig. 4. It is evident from the figure that the hardness values determined by the modified WI approach and the OP method agree reasonably well as almost all the data points fall within the area enclosed by ±5% error lines.

A blunt indenter may behave as a perfectly sharp indenter, if the penetration depth is sufficiently large in comparison to the tip radius [14]. If this condition prevails, the experimental loading curve can be approximated by $P = Ch^2$. It has been found that the loading curves reported in the literature [1,20,21] are indeed describable by such relation and, therefore, can be used as the representative experimental data pertaining to an ideally sharp indenter for validation. Materials considered herein include: aluminum, quartz, soda lime glass, fused silica, sapphire, tungsten, copper, steel, and silicon nitride. These materials are selected due to the fact that the set exhibits a wide range of conventional hardness values, H_{OP}, from 0.21 to 26 GPa. The load–displacement curves obtained in those studies were acquired with peak indentation loads greater than 100 mN using a Berkovich indenter. Total work done is evaluated numerically as the area under loading curves that are digitized from the literature mentioned. For all the materials listed, conventional hardness values are computed according to both modified WI approach and OP method as summarized in Table 2. As can be seen, except in the case of tungsten, the difference between $K_N H_N$ and H_{OP} is negligibly small and, thus, revalidates the proposed relation between the nominal and conventional hardness values. Although the relative percentage error for tungsten is over 16%, a value of 4.42 GPa for conventional hardness is still reasonable.

Above validation is limited to the case where no dwelling phase is present in the load–displacement curves. The dwelling phase introduces an additional term in the expression for total work done, which poses difficulty to derive a closed form solution for the hardness correction factor. However, an expression for a correction factor which takes the amount of work done during

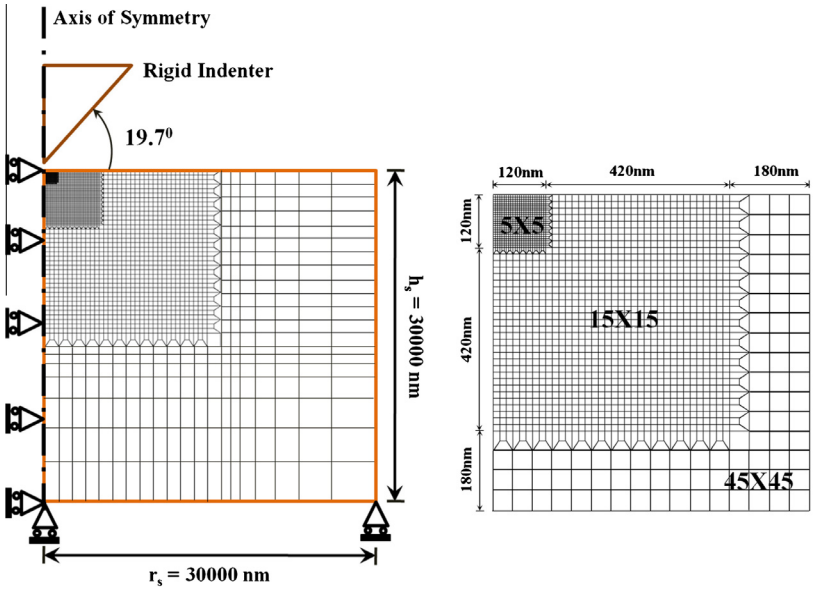

Fig. 3. The axisymmetric finite element model used in this study: (a) specimen size, discretization scheme and boundary conditions; and (b) mesh size in the vicinity of contact.

Table 1
Summary of the model parameters used in the finite element simulations of the nanoindentation load–displacement curves and their values.

Parameter	Values
Young' modulus, E (GPa)	25–410
Poisson's ratio, ν	0.25
Yield strength, σ_y (GPa)	1–20
Plastic modulus, E_P (GPa)	0, $5\sigma_y$
Coefficeint of friction	0.4
Maximum depth of penetration, h_{max} (nm)	200–250
Half included angle of Indenter, θ (°)	70.3

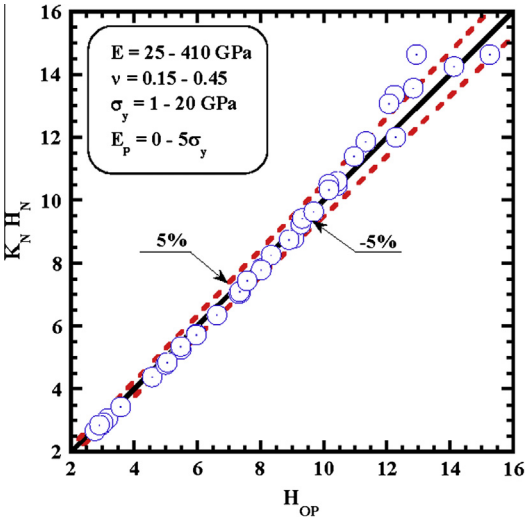

Fig. 4. Comparison of the conventional hardness evaluated by the modified work-of-indentation approach with that obtained by the standard Oliver and Pharr method using simulated indentation data.

dwelling into account could be derived empirically. For this purpose, the nanoindentation data for NiO–YSZ, Ni–YSZ and YSZ as reported in the paper by Xiang et al. [9] are chosen. These data are acquired with peak indentation load equal to 20 mN with varying dwelling period. Like previous data set, loading curves pertaining to these materials are also describable by a parabolic relation. Note that the conventional hardness values and the elastic energy constant for NiO–YSZ, Ni–YSZ and YSZ fall in the range 2–15 GPa and 2.80–6.38, respectively. It may be intuitively stated that the total work done during dwelling is proportional to $h_{max} - h_L$ (or h_L/h_{max}), where h_L is the penetration depth at which the increase in the loading ceases. If this is the case, then $K_N H_N/H_{OP}$ would be a linear function of h_L/h_{max}. With this assumption, the hardness ratio $K_D = K_N H_N/H_{OP}$ is plotted as a function of h_L/h_{max} as shown in Fig. 5. As expected, their relationship is linear, which may be written approximately as:

$$K_D = 5.09 - 4.08\frac{h_L}{h_{max}}. \tag{9}$$

Note that the above equation does not include the outlier appearing in the figure. When $h_L \to h_{max}$, $K_D \to 1.0$ which corresponds to the case of no dwelling phase in the load–displacement curve. With the development of Eq. (9), the modified work-of-indentation approach may be expressed in the following form.

$$H_W = K_N K_D \frac{kP^3_{max}}{9W_T^2} \tag{10}$$

A quantitative comparison of H_{OP} with each of H_N (red[1] markers) and H_W is depicted in Fig. 6 for NiO–YSZ, Ni–YSZ and YSZ. Note that the hardness H_W is evaluated with (green markers) and without (blue markers) considering the dwelling correction factor K_D. As can be seen, a good correlation between H_{OP} and H_W is obtained only when the total work done during dwelling is properly accounted for.

It has been shown elsewhere [22] that the elastic energy constant and fraction of penetration depth, h_f/h_{max}, recovered upon unloading are empirically related thereby indicating that a correlation between the hardness ratio K_N and h_f/h_{max} is also possible. In an effort to obtain such a correlation, K_N is plotted against h_f/h_{max} for all the materials considered in this study and is depicted in Fig. 7. As can be seen, K_N decreases exponentially with the increase

[1] For interpretation of color in Fig. 6, the reader is referred to the web version of this article.

Table 2
Calculation showing the comparison between the conventional hardness values determined by the Oliver and Pharr method and modified work-of-indentation approach.

Material	P_{max} (mN)	h_{max} (nm)	λ_E	H_W (GPa)	H_{OP} (GPa)	Relative error (%)
Aluminum	118.32	4999.0	79.3	0.20	0.21	6.8
Quartz	118.48	905.0	2.3	11.17	11.24	0.6
Soda Lime Glass	118.37	1116.7	3.0	6.03	5.9	−2.2
Fused Silica	118.50	1026.5	2.3	8.76	8.4	−4.3
Sapphire	118.43	521.0	3.1	27.34	26.9	−1.6
Tungsten	118.43	1075.7	18.6	4.42	3.8	−16.2
Copper	100.00	2100.0	24.9	0.96	0.97	0.6
1070 Steel	100.00	739.5	5.0	9.47	9.5	0.3
Silicon Nitride	100.00	501.0	2.9	25.71	25.7	−0.1

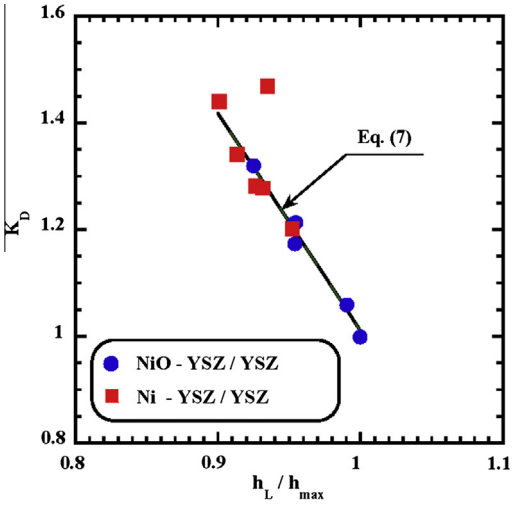

Fig. 5. Plot depicting a linear relationship between dwelling correction factor, K_D and h_L/h_{max} ratio obtained from nanoindentation data pertaining to component materials of SOFC's.

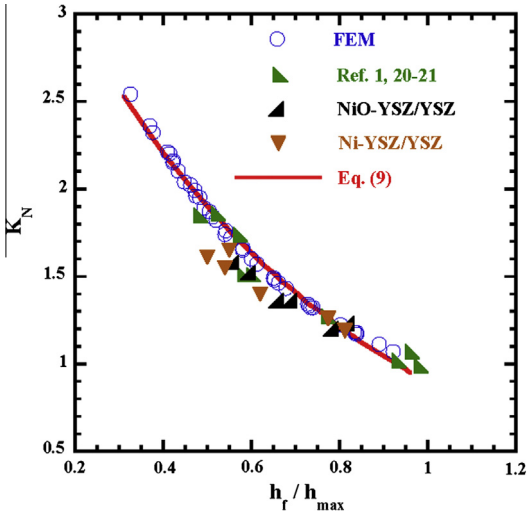

Fig. 7. Plots showing the empirical correlation between the ratio of residual to maximum penetration depths and the hardness conversion factor.

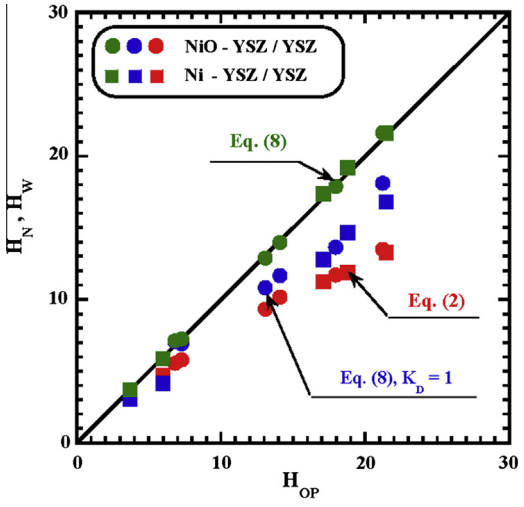

Fig. 6. Comparison of nominal hardness (H_N) and conventional hardness (H_W, with and without dwelling correction factor, K_D) evaluated by the modified work-of-indentation approach with that obtained by the Oliver and Pharr method for the component materials of SOFC.

in h_f/h_{max}; this trend may be expressed, to a good approximation, in the following form:

$$K_N = 4.0 \exp\left(-1.50 \frac{h_f}{h_{max}}\right) \quad (11)$$

Note that the above equation has a correlation coefficient of 0.9953. Only four parameters, i.e. P_{max}, h_{max}, h_L and h_f are needed to evaluate the hardness by the modified work-of-indentation approach if K_N is evaluated using Eq. (11). As these quantities can be readily obtained from the nanoindentation load–displacement curves, Eq. (11) simplifies the proposed procedure to a great extent. On the other hand, the OP method, in addition to P_{max}, h_{max} and h_f, requires the initial unloading (contact) stiffness and geometric factor to be known. The contact stiffness is generally evaluated by analytical differentiation of power law obtained by fitting the experimental unloading curve, which is often reported to be very cumbersome [22].

From the above discussion it is now clear that the proposed method is straightforward and provides the hardness value with the same level of accuracy as that given by the OP method, but with minimal computational effort. This is particularly advantageous when the nanoindentation is carried out on the heterogeneous materials. Although present study explains some fundamental issues concerning the work-of-indentation approach conclusively and expands its domain of application considerably, further refinement is needed so as to include the effects of material's pile-up and sink-in and indenter tip bluntness on the measured hardness. This will require a great deal of time, effort and simulated as well as experimental load–displacement data from different materials and, therefore, those issues are not included herein. Again, the evaluation of hardness of a material by nanoindentation is becoming extensive day by day; the technique, initially limited to rather homogenous materials, is now being applied to soft biological and stiff hard coating materials where the determination of the contact area or the analysis of unloading

curve is often infeasible. It has been reported that the elastic modulus and the hardness of a material may also be determined from the nanoindentation loading curves [20,23,24]. However, the main limitation of the loading curve method is that one of these properties must be known in advance to determine the other and, from that perspective, the modified work-of-indentation presented herein holds even greater promise.

4. Conclusion

In summary, it is generally observed that the hardness of a material determined by the OP method and the work-of-indentation approach differs remarkably. The discrepancy between the hardness values obtained by these two procedures increases as a material moves from softer to harder side on a hardness scale. The reason for such discrepancy is explained in this study using an energy-based relationship between the contact depth and the maximum depth of penetration. It has been shown that the work-of-indentation provides a nominal hardness of a material, which is fundamentally different from the conventional hardness obtained by the OP method. A relationship between the nominal and conventional hardness values is derived for an ideally sharp pyramidal indenter; their ratio is found to be a function of the elastic energy constant defined as the normalized elastic energy recovered after the complete withdrawal of load by the absolute work. The expression is validated using the load–displacement data obtained by the finite element simulation of the indentation contact on materials with a wide range of mechanical properties. The effectiveness of the proposed method is also examined with the real nanoindentation data from ceramics oxide and metals acquired with peak indentation load varying in the range 20–120 mN. An excellent agreement between the computed and experimental (OP) hardness values indicates that the proposed method is also applicable in the case of a blunt indenter provided the tip radius is very small as compared to the maximum depth of penetration. It is emphasized here that a correction is required when the experimental load–displacement data contains a dwelling phase to account for the extra work done during dwelling. The modified WI approach can be simplified further by expressing the elastic energy constant in terms of the ratio of the residual depth to the maximum depth of penetration, which can be readily obtained from the load–displacement curves of a material. Although the modification applied to the existing work-of-indentation approach expands the domain of its application considerably, a further study is required to test the accuracy of the modified approach for a material that shows excessive 'pile-up' and 'sink-in' during indentation and for an indenter with large tip radius in comparison to the maximum penetration depth.

Acknowledgements

KKJ acknowledges the financial support in the form of Dissertation Year Fellowship (DYF) from the University Graduate School, Florida International University.

References

[1] W.C. Oliver, G.M. Pharr, J. Mater. Res. 7 (1992) 1564–1583.
[2] J.R. Tuck, A.M. Korsunsky, S.J. Bull, R.I. Davidson, Surf. Coat. Technol. 137 (2001) 217–224.
[3] I.N. Sneddon, Int. J. Engng. Sci. 3 (1965) 47–57.
[4] F.-J. Ulm, M. Vandamme, C. Bobko, J.A. Ortega, K. Tai, C. Ortiz, J. Am. Ceram. Soc. 90 (2007) 2677–2692.
[5] D. Beegan, S. Chowdhury, M.T. Laugier, Surf. Coat. Technol. 192 (2005) 57–63.
[6] M.K. Khan, S.V. Hainsworth, M.E. Fitzpatrick, L. Edwards, J. Mater. Sci. 44 (2009) 1006–1015.
[7] L. Zhou, Y. Yao, Mater. Sci. Eng. A 460–461 (2007) 95–100.
[8] O. Uzun, N. Guclu, U. Kolemen, O. Sahin, Mater. Chem. Phys. 112 (2008) 5–15.
[9] Z. Xiang, W. Fenghui, J. Power Sources 201 (2012) 231–235.
[10] Y. Cao, Z. Xue, X. Chen, D. Raabe, Scripta Mater. 59 (2008) 518–521.
[11] D. Ma, C.W. Ong, T. Zhang, Exp. Mech. 49 (2009) 719–729.
[12] M.T. Attaf, Mater. Lett. 58 (2004) 889–894.
[13] K.K. Jha, N. Suksawang, D. Lahiri, A. Agarwal, ACI Mater. J. 109 (2012) 81–90.
[14] K.K. Jha, S. Zhang, N. Suksawang, T. Wang, A. Agarwal, J. Phys. D: Appl. Phys. 46 (2013) 415501–415511.
[15] B. Poon, D. Rittel, G. Ravichandran, Int. J. Solids Struct. 45 (2008) 6018–6033.
[16] J.C. Hay, A. Bolshakov, G.M. Pharr, J. Mater. Res. 14 (1995) 2296–2305.
[17] J.A. Knapp, D.M. Follstaed, S.M. Myres, J.C. Barbour, T.A. Friedmann, J. Appl. Phys. 85 (1995) 1460–1474.
[18] Z.H. Xu, X. Li, Acta Mater. 56 (2008) 1399–1405.
[19] J.M. Meza, F. Abbes, M. Troyon, J. Mater. Res. 23 (2008) 725–731.
[20] S.V. Hainsworth, H.W. Chandler, T.F. Page, J. Mater. Res. 11 (1996) 1987–1995.
[21] S. Jayaraman, G.T. Hahn, W.C. Oliver, C.A. Rubin, P.C. Bastias, Int. J. Solids Struct. 35 (1998) 365–381.
[22] K.K. Jha, N. Suksawang, D. Lahiri, A. Agarwal, J. Mater. Res. 28 (2013) 789–797.
[23] J. Malzbender, G. de Width, J. den Toonder, J. Mater. Res. 15 (2000) 1209–1212.
[24] K.K. Jha, N. Suksawang, A. Agarwal, Scripta Mater. 63 (2010) 261–264.